Solid Earth Discuss., 6, 2293–2320, 2014
www.solid-earth-discuss.net/6/2293/2014/
doi:10.5194/sed-6-2293-2014

Solid Earth Discussions
Open Access

Characterisation of the magmatic signature in gas emissions from Turrialba volcano, Costa Rica

Y. Moussallam[1], N. Peters[1], C. Ramírez[2], C. Oppenheimer[1], A. Aiuppa[3,4], and G. Giudice[4]

[1]Department of Geography, University of Cambridge, Downing Place, Cambridge, CB2 3EN, UK
[2]Red Sismológica Nacional, University of Costa Rica (UCR), San Jose, Costa Rica
[3]Dipartimento DiSTeM, Università di Palermo, Via archirafi 36, 90146, Palermo, Italy
[4]Instituto Nazionale di Geofisica e Vulcanologia, Sezione di Palermo Via La Malfa, 153, 90146, Palermo, Italy

Received: 15 July 2014 – Accepted: 22 July 2014 – Published: 8 August 2014

Correspondence to: Y. Moussallam (yves.moussallam@cnrs-orleans.fr)

Published by Copernicus Publications on behalf of the European Geosciences Union.

Abstract

The equilibrium composition of volcanic gases with their magma is often overprinted by interaction with a shallow hydrothermal system. Identifying the magmatic signature of volcanic gases is critical to relate their composition to properties of the magma (temperature, fO_2, gas-melt segregation depth). We report measurements of the chemical composition and flux of the major gas species emitted from Turrialba volcano during March 2013. Measurements were made of two vents in the summit region; one of which opened in 2010 and the other in 2012. We determined an average SO_2 flux of $2.40 \pm 0.75\,kg\,s^{-1}$ using scanning ultraviolet spectroscopy, and molar proportions of H_2O, CO_2, SO_2, HCl, CO and H_2 gases of 94.16, 4.03, 1.56, 0.23, 0.003 and 0.009 %, respectively, by open-path Fourier transform infrared (FTIR) spectrometry and a multi-species gas sensing system. Together, these data imply fluxes of 41, 4, 0.2, 2×10^{-3} and $5 \times 10^{-4}\,kg\,s^{-1}$ for H_2O, CO_2, HCl, CO and H_2 respectively. Although H_2S was detected, its concentration could not be resolved. HF was not detected. The chemical signature of the gas from both vents was found to be broadly similar. Following the opening of the 2010 and 2012 vents we found limited to negligible interaction of the magmatic gas with the hydrothermal system has occurred and the gas composition of the volcanic plume is broadly representative of equilibrium with the magma. The time evolution of the gas composition, the continuous emission of large quantities of SO_2 and the physical evolution of the summit area with new vent opening and more frequent eruptions all point towards a continuous drying of the hydrothermal system at Turrialba's summit at an apparently increasing rate.

1 Introduction

Measurement of gas emissions from volcanoes in a state of unrest can provide valuable information regarding the evolution of the magmatic system and play a key role in eruption forecasting strategies (e.g. Merapi, 2010 crisis; Surono et al., 2012). In recent

SED
6, 2293–2320, 2014

years tremendous progress in instrumentation has been made with the development of miniature UV spectrometers (e.g. Oppenheimer, 2010), Open-path Fourier transform infrared (FTIR) spectroscopy (e.g. Horrocks et al., 2001) and multi-species gas sensing systems (e.g. Aiuppa et al., 2006) making rapid measurement of all major gas species a relatively straightforward endeavour given favourable conditions.

Turrialba volcano is located at the southern tip of the "Cordillera Central" (Fig. 1) a Holocene volcanic belt formed by the subduction of the Cocos Plate beneath the Caribbean Plate. Turrialba lies 35 km away from San José and 15 km away from Cartago, the first and second largest cities in Costa Rica. Since its last major eruption in 1884–1886 (Reagan et al., 2006), the volcano has been passively degassing via a rapidly changing fumarolic system (Vaselli et al., 2010). Three craters make up the summit area of Turrialba; the East crater, Central crater and West crater. The fumarole activity is concentrated around the West crater in three main regions (Fig. 2); the Northern fumarole field, the 2010 vent and 2012 vent. At the time of our fieldwork in March 2013, gas emitted from the 2012 vent reached up to 700–800 °C, while gas emitted from the 2010 vent was up to 400 °C. These temperatures were measured using a hand-held thermal camera (at a range of ~ 350 m and ~ 20 m respectively) and were not corrected for atmospheric transmission. These thus indicate minimum estimates of the true gas temperature.

Following an episode of intense fumarolic activity in 2008 and persistent acid rain ever since, the vegetation within a 1 to 2 km radius of the summit has been strongly affected (Martini et al., 2010). Livestock have also been affected and a large portion of the local population has left the area after suffering economic losses or health issues (Martini et al., 2010). On 5 January 2010, a small phreatic eruption opened a new vent (2010 vent) and resulted in ash falls reaching the suburbs of San José (OVSICORI 2010; González et al., 2014). On 12 January 2012, a new vent opened on the south east flank of the West Crater and ash fell as far as Tres Rios (27 km SW from the vent) (OVSICORI 2012; González et al., 2014). The national park of Turrialba closed following this event and has remained so since. On 21 May 2013, an eruption from the 2010

SED
6, 2293–2320, 2014

and 2012 vents resulted in ash falls more than 40 km away (OVSICORI 2013; Red Sismologica Nacional, 2013). The recent change in the style of degassing together with the increasing frequency of minor ash eruptions underlines the importance of investigation of the composition of the gas emissions, in order to understand the evolution of the magma-hydrothermal system.

Here we report measurements of the gas emissions from the 2010 and 2012 vents at Turrialba volcano using (i) scanning ultraviolet differential optical absorption spectroscopy (DOAS) (ii) open-path FTIR spectroscopy and (iii) multi-species gas sensing systems ("multi-gas"). Reported measurements of the gas chemistry and flux at Turrialba have been few and sporadic. Vaselli et al. (2010) characterised the change in gas composition of fumaroles from the hydrothermal system from 1998 to 2008 while (Martini et al., 2010) and Campion et al. (2012) reported measurement of the SO_2 flux from 2002 to 2008 and 2009 to 2011 respectively. The opening of the 2010 vents and associated increase in SO_2 flux was interpreted as the beginning of open vent degassing (Campion et al., 2012). The present investigation spans a period from 22–26 March 2013. The aim of this investigation is to provide measurements of the magmatic gases emitted from Turrialba at an early stage in its new open-vent style activity in order to provide a reference point for future investigations of the gas emissions from this potentially hazardous volcano. Such studies, especially if they are repeated, are important in identifying the evolution of volcanic unrest, particularly in the case of reactivation of long-dormant volcanoes.

2 Methods

2.1 Scanning DOAS

Horizontal scans transecting the plume just above the crater were made from a site 2 km away from the summit. The plume rose vertically to approximately 400 m before drifting horizontally with the wind, such that scans always cleared the plume on

SED
6, 2293–2320, 2014

both sides. Data acquisition was paused whenever cloud formed within the field of view. The acquisition of data and subsequent retrieval of SO_2 flux values followed the standard DOAS methodology (Galle et al., 2003; Platt and Stutz, 2008). Scans were taken by mounting a telescope (coupled to the spectrometer by a fibre) on a small, custom-made, USB-powered scanning stage. The spectrometer recorded continuously as the stage was rotated back and forth and angles were assigned to each spectrum in post-processing using their timestamps (recorded with millisecond precision) and an angle-versus-time log file created by the scanning software (code available at: http://code.google.com/p/avoscan/). Rise speeds for the plume were estimated using a dual wide field of view (DW-FOV) spectrometer system similar to that described by (Boichu et al., 2010). This was operated alongside the scanning unit, and data from the two telescopes were cross-correlated using a window length of 300 s to determine the rise speed. We used the solar spectrum measured by (Chance and Kurucz, 2010) and SO_2 and O_3 reference spectra measured by Vandaele et al. (1994) and Burrows et al. (1999), respectively. All DOAS retrievals were implemented using a combination of the DOASIS software (https://doasis.iup.uni-heidelberg.de) and scripts written by Vitchko Tsanev (http://www.geog.cam.ac.uk/research/projects/doasretrieval/).

The scanning stage uses a stepper motor with a 99 : 1 planetary gearbox, giving it an accuracy of ±0.01°. Note that errors due to crash-back in the gearbox are systematic for a single scan, and therefore do not affect the integrated column amount. The precision of the timestamps in the spectrum files (millisecond) has a small effect on the accuracy of the angles. Using Eq. (1) and the standard error propagation equation the error in the angle (δ_{θ_τ}) of a spectrum recorded at time τ can be calculated by:

$$\delta_{\theta_\tau} = |\theta_\tau| \cdot \sqrt{\delta_\theta^2 + \left((\tau - \tau_0) \cdot \frac{\mathrm{d}\theta}{\mathrm{d}t}\right)^2 \cdot \left(2\delta_\theta^2 + \frac{\delta_\tau^2}{(\tau - \tau_0)^2}\right)} \quad (1)$$

where $\delta_\theta = 0.01°$ is the uncertainty in the angle of the stepper motor and $\delta_\tau = 0.001$ s is the uncertainty in the capture time of the spectrum.

SED
6, 2293–2320, 2014

Error in the retrieved SO_2 column amount is estimated by the DOASIS software by analysing the residual from the fitting of the reference and Ring spectra. Propagating these errors along with those in the angles through Eq. (2) gives the following as an estimate of the error in the flux (δ_Φ):

$$\delta_\Phi^2 = \Phi^2 \left[\left(\frac{k v \delta_{\mathrm{ICA}}}{\Phi} \right)^2 + \left(\frac{\delta_v}{v} \right)^2 \right] \tag{2}$$

where $\delta_v = 1\,\mathrm{m\,s^{-1}}$ is the uncertainty in the plume rise speed (corresponding to one standard deviations on measured rise speed) and δ_{ICA} is the error in the integrated column amount given by:

$$\delta_{\mathrm{ICA}}^2 = \sum_{i=0}^{n-1} A_i^2 \left[\left(\frac{\sqrt{\delta_{\theta i}^2 + \delta_{\theta i+1}^2}}{\theta_{i+1} - \theta_i} \right)^2 + \left(\frac{\sqrt{\delta_{Ai}^2 + \delta_{Ai+1}^2}}{A_{i+1} - A_i} \right)^2 \right] \tag{3}$$

2.2 FTIR spectroscopy

Open-path FTIR measurements were made on 25 and 26 March 2013. The spectrometer (MIDAC M4411-S) was equipped with a Stirling-cooled MCT detector and a 3 inch telescope. We collected interferograms with a nominal optical path difference (retardation) of 2.0 cm corresponding to a spectral resolution of $0.5\,\mathrm{cm^{-1}}$. On 25 March, the spectrometer was pointing directly at the 2012 vent, using it as the infrared radiation source (optical path length ~ 350 m). During acquisition, gases emitted from the 2012 vent were rising straight up at high velocity (observed with a thermal camera) such that volcanic gas plume was approximately 2 m thick. On 26 March a 15 cm-diameter infrared lamp provided the source of radiation and was positioned ~ 35 m from the spectrometer, both deployed on the southern edge of the western crater, directly south of the 2010 vent. Measurements were collected as the plume passed through the optical

SED
6, 2293–2320, 2014

path. Interferograms were collected at ~ 1 Hz. Raw interferograms were inverse Fourier transformed to yield single beam spectra using a Mertz phase correction and triangular apodization. Column amounts of H_2O, CO_2, CO, SO_2 and HCl were retrieved from their absorption fingerprint in single beam spectra using a well-tested code (Burton et al., 2007, 2000; Horrocks et al., 2001) that simulates and fits atmospheric transmittance in discrete wavebands. Fitting parameters are given in Table 1.

2.3 In situ gas measurements

Electrochemical and non-dispersive infrared (NDIR) sensors ("multi-gas") measurements were performed on 24, 25 and 26 March at a sample rate of 0.5 Hz. The instrument was deployed on the southern edge of the western crater, directly south of the 2010 vent at an altitude of 3280 m a.s.l. On 25 March the instrument was located a few meters away from the IR lamp. The multi-gas instrument incorporated H_2, H_2S, CO and SO_2 electrochemical sensors, a NDIR sensor for CO_2, and a sensor for temperature and humidity measurements. In this type of instrument, the sampled gas is circulated via a miniature 12 V rotary pump through the sensors (e.g. Aiuppa et al., 2011). This instrument, including the electrochemical sensors it contains is the same unit that has been previously deployed at Erebus volcano (Antarctica) and is described in detail by (Moussallam et al., 2012).

All sensors were calibrated in the laboratory on 5 February 2013 with target gases of known concentration. The response time of all sensors was rapid but the H_2, H_2S and CO sensors were found to respond more slowly than SO_2 and CO_2 sensors (see Fig. S1). The differences in response time for the different sensors were corrected by finding the lag times from correlation analysis of the various time series.

SED
6, 2293–2320, 2014

3 Results

3.1 SO_2 flux

Emission rates of SO_2 are shown in Fig. 3 as flux in kg s^{-1} and t d^{-1} for measurements made on the 22, 23 and 25 of March 2013. We report only fluxes obtained during cloud-free periods where the plume was well defined and was cleared by the scan on both sides. The average SO_2 emission rate on 22 March is 4.0 ± 0.5 kg s^{-1} (equivalent to 350 ± 50 t d^{-1}), on 23 March is 2.3 ± 0.5 kg s^{-1} (equivalent to 200 ± 45 t d^{-1}) and on 25 March is 2.1 ± 0.5 kg s^{-1} (equivalent to 190 ± 40 t d^{-1}) giving a three day average of 2.4 ± 0.7 kg s^{-1} (equivalent to 210 ± 65 t d^{-1}).

3.2 Chemistry

3.2.1 Multi-gas

We obtained 6.8 h of good quality observations of the 2010 vent chemistry using the multi-gas instrument. H_2 and H_2S sensors were found to be sensitive to changes in temperature, drifting strongly at temperature above 26 °C. We therefore only report 2.1 h of H_2 measurements which were acquired at sampled air temperatures between 20 and 25 °C, close to the laboratory calibration temperature. The H_2S signal was strongly dominated by its 10–15 % cross-correlation with SO_2 and after correction H_2S was not detected. CO was likewise not detected by the electrochemical sensor. Figure 4 shows four scatter plots for continuous measurements acquired on 24–26 March. Scatter plots for the CO_2 and SO_2 measurements yield CO_2/SO_2 molar ratios varying between 1.66 and 1.79 (Fig. 4a–c), with a weighted average of 1.76. The H_2 and SO_2 scatter plot (Fig. 4d) measurements yield a H_2/SO_2 molar ratio of 0.006. It is to be noted that the hydrogen level above atmospheric background is very weak and hence has a large associated error. The significant scattering seen in the Multi-gas data is not solely a reflection of the measurement error but also reflects the variability

SED
6, 2293–2320, 2014

of the gas sampled. Indeed while the largest contributor to the analysed gas plume appeared to be the 2010 vent, contributions from the 2012 vent, nearby low temperature fumaroles and occasionally the northern fumarolic field are likely. The reported multi-gas measurements are therefore an approximation of the bulk plume composition and not strictly a reflection of the gas chemistry of the 2010 vent.

3.2.2 FTIR

A total of 2162 spectra were collected on 26 March and analysed for H_2O, CO_2, SO_2, CO, HCl, HF, CH_4 and N_2O. Figure 5a–d shows the scatter plots for CO, CO_2, H_2O and HCl column amount plotted against SO_2. A total of 3983 spectra for the 2012 vent plume were collected on 25 March and analysed for the same species. Figure 5e–g shows the column amount scatter plots for CO_2, H_2O and HCl plotted against SO_2. The scatter is much greater in measurements of the 2012 vent due to the passive sensing field setup (short path-length of gas relative to total path-length and low infrared source strength) and contamination of the absorption signal by IR radiation from the hot gases. The latter issue made it particularly difficult to make useful measurements and all retrievals showing unreasonable amounts (e.g. negative) of HCl and H_2O were dismissed. Column amounts of CH_4 and N_2O were stable throughout the measurement period indicating that these species were present in the ambient atmosphere but were not detected in the plume. HF was not detected in any of the spectra and CO was below the detection limit for measurements of the 2012 vent emissions, possibly due to the short path-length of gas relative to the total path-length but most probably due to the low energy from the source. The CO_2 intercept of 2.19×10^{20} molecules cm^{-2}, from Fig. 5e, corresponds to an atmospheric mixing ratio of 364 ppmv over a 350 m path length, which agrees reasonably well with the expected ambient abundance of CO_2. Similarly the CO_2 intercept of 2.05×10^{19} molecules cm^{-2}, from Fig. 5b, corresponds to an atmospheric mixing ratio of 336 ppmv over a 35 m path length (based on an ambient air temperature of 290 K and a pressure of 700 hPa).

SED
6, 2293–2320, 2014

By converting the molar ratios of volcanic gas species illustrated in Figs. 4 and 5 to mass ratios and multiplying by the average SO_2 flux obtained from scanning DOAS, we can estimate emission rates of each individual gas from Turrialba. We obtained fluxes of 41, 4, 0.2, 2×10^{-3} and 5×10^{-4} kg s^{-1} for H_2O, CO_2, HCl, CO and H_2 respectively (Table 2) with associated error of ± 12, 1.2, 0.7, 0.06, 6×10^{-4} and 1×10^{-4} kg s^{-1} for H_2O, CO_2, HCl, CO and H_2 respectively (based on error from SO_2 flux measurement).

4 Discussion

4.1 Gas flux

Few measurements of SO_2 emissions from Turrialba have been published so far; (Martini et al., 2010) reported SO_2 fluxes increasing from 0 to ~ 10 kg s^{-1} from 2002 to 2008. Campion et al. (2012) reported SO_2 fluxes between < 5 kg s^{-1} and 9 kg s^{-1} between September and October 2009, i.e. before the 5 January 2010 eruption, followed by SO_2 fluxes of up to 58 kg s^{-1} directly after the eruption, decreasing linearly with time down to 18 kg s^{-1} by January 2011. Conde et al. (2014) reported SO_2 fluxes between 8 and 11 kg s^{-1} a week prior to our investigation. The average SO_2 emission rate data for three days of measurements in March 2013 is 2.4 ± 0.7 kg s^{-1} (equivalent to 210 ± 65 t d^{-1}). This is comparable to the lowest values recorded by previous investigations but indicates the sustained emission of a significant amount of sulphur to the atmosphere from the volcano. The fluxes of other species (CO_2 excepted, Table 2), are the first such measurements to be reported since the opening of the 2010 and 2012 vents. Fluxes of H_2O and CO_2 are about ten time lower and HCl flux is 40 times lower than the flux measured in nearby Masaya volcano in 1998–1999 (Nicaragua; Burton et al., 2000).

SED
6, 2293–2320, 2014

4.2 Gas composition

While the Multi-gas instrument deployed directly south of the 2010 vent records a CO_2/SO_2 molar ratio of 1.76, the FTIR spectrometer, located a few meters to the east, yields a CO_2/SO_2 molar ratio of 2.59. This discrepancy can be fully attributed to unequal degrees of contribution from the Northern fumarolic field. Indeed the Multi-gas instrument, located slightly further to the west compared to the FTIR-lamp setup is likely to be more affected by the fumaroles' emissions. Future field campaigns should try to avoid this issue by deploying these instruments further to the east. We note that the CO_2/SO_2 molar ratio we obtained are within error of the one reported by Conde et al. (2014) (CO_2/SO_2 molar ratio of 1.96 to 2.98) during their investigation earlier in the same month.

The resemblance in chemistry, with near similar H_2O/SO_2 and HCl/SO_2 molar ratio (Table 2) between the mixed plume (dominated by degassing from the 2010 vent) and the 2012 vent suggests a common magmatic source. This has been made apparent by the May 2013 eruption, in which both vents emitted ash (Fig. 7b). However, there are some differences, most evident in the C/S ratios between the 2010/mixed plume and the 2012 vent with a CO_2/SO_2 molar ratio of 2.59 in the mixed plume compared to 7 in the 2012 vent. This difference might simply reflect the large error in the passive FTIR measurements. Indeed imposing a regression through a 400 ppm CO_2 background would yield a CO_2/SO_2 ratio of 2 ($R^2 = 0.12$), identical to the measured ratio of 2 at the 2010 vent with active source. If the slight difference in chemistry is real however, one possible scenario explaining the higher C/S ratio for the 2012 vent is a more efficient scrubbing of SO_2 in the 2012 vent or conversely, more efficient removal of CO_2 from the 2010 vent emissions. However, we discard this hypothesis as the 2010 and 2012 vent emissions were at least 400 °C and 750 °C, respectively, i.e. higher than the temperature at which scrubbing operates (Gerlach et al., 2008; Symonds et al., 2001). More efficient scrubbing of CO_2 than SO_2 is particularly unlikely as discussed in Gerlach (2008). Another scenario is that gases emitted from the

SED
6, 2293–2320, 2014

2012 vent reflect equilibrium with a deeper level of the magma hence higher C / S and S / Cl and lower H_2O / CO_2. This hypothesis is consistent with the observation that gas emitted from the 2012 vent is more pressurized than that from the 2010 vent. This last point however could also simply reflect different vent geometry (small vent compared to the flux). Lastly the difference in chemistry might reflect contamination of our 2010 vent chemistry estimate by contribution from the Northern fumarolic field. Our preferred conclusion, given the limited dataset, is that the apparent difference in the C / S ratio between the two vents is solely a reflection of the high error on the 2012 vent measurements.

Table 3 compares the mixed plume chemistry from Turrialba to that of other arc volcanoes. The Turrialba plume chemistry most closely resembles that of the Nicaraguan volcanoes (Momotombo and Masaya), especially Masaya. The SO_2 / HCl molar ratio is much higher than that measured at other arc volcanoes presented here (7.8 compared to an average of 1.5) and is closer to volcanoes such as Etna and Surtsey (10 and 6.2 respectively; Allard et al., 2005; Gerlach, 1980).

4.3 Oxygen fugacity

The oxygen fugacity of the degassing magma can be estimated using the measured CO_2 / CO molar ratio of 1334 from the mixed plume based on the reaction:

$$CO + 1/2O_2 = CO_2 \quad (4)$$

At atmospheric pressure, the fugacity of a gas is equal to its partial pressure (assuming ideal behaviour, which is reasonable for atmospheric pressure) and the oxygen fugacity can be calculated as:

$$f_{O_2} = \left(K \frac{x_{CO_2}}{x_{CO}} \right)^2$$

SED
6, 2293–2320, 2014

where x_i the mole fraction of the ith species and K is the equilibrium constant for Eq. (4) and is related to the change in Gibbs' free energy via:

$$K = \exp(-\Delta G/RT)$$

where R is the gas constant and T the temperature. The change in Gibbs' free energy (ΔG) can be computed from the thermochemical JANAF tables for a large range of temperatures. Since the temperature of the magma is unknown we used an estimated temperature for the suspected andesite to basaltic-andesite magma. Estimated temperatures of 900 °C, 1000 °C and 1100 °C yield fO_2 values of 2.8, 2.9 and 3.1 log units above the QFM buffer, respectively. In the temperature range considered, using the measured H_2O/H_2 ratio would yield fO_2 estimates about 4 log units above the QFM buffer. Because the H_2O/H_2 ratio is obtained using the Multi-gas instrument, which as mentioned above shows a greater amount of contamination from the Northern fumarolic field and since non-magmatic H_2O cannot be excluded, we regard the fO_2 estimate from the CO_2/CO ratio as more robust. The oxidized fO_2 measured in the gas emissions corresponds to equilibrium conditions with the magma at shallow level and is fairly typical, although slightly high, for arc volcanoes. At Masaya volcano, the matrix glass from basaltic scoria record close, yet slightly more reduced conditions at 1.4 to 2.3 ± 0.2 log units above the QFM buffer (de Moor et al., 2013).

4.4 Current state of the degassing

Vaselli et al. (2010) reported substantial changes in gas composition of fumaroles in the summit area from 1998 to 2008 with the detection of SO_2 in 2002 and a constant change in gas chemistry (increasing S/CO_2 and $(HF + HCl)/CO_2$ ratio) since then. They interpreted this change from low temperature hydrothermal-dominated to high temperature magmatic-dominated chemistry to be related to a cyclic evolution of the hydrothermal system. Since then the 2010 vent opened, releasing 1 ± 0.3 Tg of SO_2 from January 2010 to January 2011 (Campion et al., 2012). Subsequently the 2012 vent opened up and in May 2013 both vents erupted ash (Fig. 7b). The chronology of

SED
6, 2293–2320, 2014

events and the evolution of gas emission rates and chemistry is summarised in Fig. 6. From Fig. 6 it appears that the plume chemistry we measured (in term of S/CO_2 but this is also true in term of $(HF+HCl)/CO_2$ ratio) is similar to that recorded by Vaselli et al. (2010) during the intense fumarolic activity of late 2007 to 2008. The SO_2 fluxes measured in March 2013 are similar to that measured by Campion et al. (2012) a few months prior to the 2010 phreatic eruption, which is interesting when considering that the 2013 eruption occurred two months after our measurements. Although the current dataset is too disparate to conclude with any confidence, this last point does hint of a recurring process. A conceivable scenario is that low SO_2 flux is indicative of a decrease in porosity in the upper part of the edifice, leading periodically to small scale eruptions (with or without the opening of a new vent) following pressure build-up at shallow levels.

The increasing frequency of ash eruptions, the decreasing activity of low temperature fumaroles since the opening of the 2010 and 2012 vents, the elevated (400 °C and 750 °C respectively) temperatures they show, and the very oxidized gas signature all point towards (in accordance to Campion et al., 2012; Vaselli et al., 2010) a progressive drying out of the hydrothermal system and degassing that is controlled by near open-vent processes with limited-to-negligible interaction with the hydrothermal system. This scenario is depicted in schematic form in Fig. 7a, intentionally drawn in the same style as Fig. 7 in (Campion et al., 2012) to show the evolution of the system since their investigation in 2010–2011.

5 Conclusions

We measured the composition and flux of gases emitted from Turrialba volcano in March 2013 using a scanning ultraviolet spectrometer, FTIR spectroscopy and Multi-gas sensors. The compositions measured using FTIR are largely consistent with those measured with the Multi-gas instrument, and discrepancies may be explained by differing amounts of contamination from fumaroles. The gas composition reflects magmatic

SED
6, 2293–2320, 2014

degassing with a limited contribution from hydrothermal sources, suggesting near completion of the progressive drying up of the hydrothermal system in the summit region of Turrialba volcano or isolation of these main vents from the hydrothermal system. FTIR measurements of the gas emissions from the two main vents reveals only minor difference in their chemistry. Repeated gas monitoring campaigns of the sort presented here are encouraged in order to capture the future evolution of the state of unrest at Turrialba.

The Supplement related to this article is available online at doi:10.5194/sed-6-2293-2014-supplement.

Acknowledgements. This research was supported by a fieldwork grant from the Royal Geographical Society. Y. M. and N. P. were additionally supported by the Philip Lake funds from the Department of Geography, University of Cambridge. Y. M. acknowledge a research grant from Mazamas We thank the NERC Field Spectroscopy Facility for the loan of their infrared spectrometer. We are grateful to Kayla Iacovino and Gino González-Ilama for help in the field.

References

Aiuppa, A., Federico, C., Giudice, G., Gurrieri, S., and Valenza, M.: Hydrothermal buffering of the SO_2 / H_2S ratio in volcanic gases: evidence from La Fossa Crater fumarolic field, Vulcano Island, Geophys. Res. Lett., 33, L21315, doi:10.1029/2006GL027730, 2006.

Aiuppa, A., Shinohara, H., Tamburello, G., Giudice, G., Liuzzo, M., and Moretti, R.: Hydrogen in the gas plume of an open-vent volcano, Mount Etna, Italy, J. Geophys. Res., 116, B10204, doi:10.1029/2011JB008461, 2011.

Allard, P., Burton, M., and Muré, F.: Spectroscopic evidence for a lava fountain driven by previously accumulated magmatic gas, Nature, 433, 407–410, doi:10.1038/nature03246, 2005.

Boichu, M., Oppenheimer, C., Tsanev, V., and Kyle, P.: High temporal resolution SO_2 flux measurements at Erebus volcano, Antarctica, J. Volcanol. Geoth. Res., 190, 325–336, doi:10.1016/j.jvolgeores.2009.11.020, 2010.

Burrows, J. P., Richter, A., Dehn, A., Deters, B., Himmelmann, S., Voigt, S., and Orphal, J.: Atmospheric remote-sensing reference data from GOME-2. Temperature-dependent absorb-

SED
6, 2293–2320, 2014

tion cross sections of O_3 in the 231–794 nm range, J. Quant. Spectrosc. Ra., 61, 509–517, doi:10.1016/S0022-4073(98)00037-5, 1999.
Burton, M., Allard, P., Mure, F., and La Spina, A.: Magmatic gas composition reveals the source depth of slug-driven Strombolian explosive activity, Science, 317, 227–230, doi:10.1126/science.1141900, 2007.
Burton, M. R., Oppenheimer, C., Horrocks, L. A., and Francis, P. W.: Remote sensing of CO_2 and H_2O emission rates from Masaya volcano, Nicaragua, Geology, 28, 915–918, doi:10.1130/0091-7613(2000)28<915:RSOCAH>2.0.CO;2, 2000.
Campion, R., Martinez-Cruz, M., Lecocq, T., Caudron, C., Pacheco, J., Pinardi, G., Hermans, C., Carn, S., and Bernard, A.: Space- and ground-based measurements of sulphur dioxide emissions from Turrialba Volcano (Costa Rica), B. Volcanol., 74, 1757–1770, doi:10.1007/s00445-012-0631-z, 2012.
Chance, K. and Kurucz, R. L.: An improved high-resolution solar reference spectrum for earth's atmosphere measurements in the ultraviolet, visible, and near infrared, J. Quant. Spectrosc. Ra., 111, 1289–1295, 2010.
Conde, V., Robidoux, P., Avard, G., Galle, B., Aiuppa, A., Muñoz, A., and Giudice, G.: Measurements of volcanic SO_2 and CO_2 fluxes by combined DOAS, Multi-GAS and FTIR observations: a case study from Turrialba and Telica volcanoes, Int. J. Earth Sci., 14, 223–245, doi:10.1007/s00531-014-1040-7, 2014.
De Moor, J. M., Fischer, T. P., Sharp, Z. D., King, P. L., Wilke, M., Botcharnikov, R. E., Cottrell, E., Zelenski, M., Marty, B., Klimm, K., Rivard, C., Ayalew, D., Ramirez, C., and Kelley, K. A.: Sulfur degassing at Erta Ale (Ethiopia) and Masaya (Nicaragua) volcanoes: implications for degassing processes and oxygen fugacities of basaltic systems, Geochem. Geophy. Geosy., 14, 4076–4108, doi:10.1002/ggge.20255, 2013.
Gerlach, T. M.: Evaluation of volcanic gas analysis from surtsey volcano, iceland 1964–1967, J. Volcanol. Geoth. Res., 8, 191–198, doi:10.1016/0377-0273(80)90104-3, 1980.
Gerlach, T. M. and Casadevall, T. J.: Evaluation of gas data from high-temperature fumaroles at Mount St. Helens, 1980–1982, J. Volcanol. Geoth. Res., 28, 107–140, doi:10.1016/0377-0273(86)90008-9, 1986.
Gerlach, T. M., McGee, K. A., and Doukas, M. P.: Emission Rates of CO_2, SO_2, and H_2S, Scrubbing, and Preeruption Excess Volatiles at Mount St. Helens, 2004–2005, in A Volcano Re kindled: the Renewed Eruption of Mount St. Helens, 2004–2006, Geological Survey Professional Paper 1750, 543–571, 2008.

SED
6, 2293–2320, 2014

Hammouya, G., Allard, P., Jean-Baptiste, P., Parello, F., Semet, M. P., and Young, S. R.: Pre- and syn-eruptive geochemistry of volcanic gases from Soufriere Hills of Montserrat, West Indies, Geophys. Res. Lett., 25, 3685–3688, doi:10.1029/98GL02321, 1998.

Horrocks, L. A., Oppenheimer, C., Burton, M. R., Duffell, H. J., Davies, N. M., Martin, N. A., and Bell, W.: Open-path Fourier transform infrared spectroscopy of SO_2?: an empirical error budget analysis, with implications for volcano monitoring, J. Geophys. Res., 106, 27647, doi:10.1029/2001JD000343, 2001.

Le Guern, F., Gerlach, T. M., and Nohl, A.: Field gas chromatograph analyses of gases from a glowing dome at Merapi volcano, Java, Indonesia, 1977, 1978, 1979, J. Volcanol. Geoth. Res., 14, 223–245, doi:10.1016/0377-0273(82)90063-4, 1982.

Martin, R. S., Sawyer, G. M., Spampinato, L., Salerno, G. G., Ramirez, C., Ilyinskaya, E., Witt, M. L. I., Mather, T. A., Watson, I. M., Phillips, J. C., and Oppenheimer, C.: A total volatile inventory for Masaya Volcano, Nicaragua, J. Geophys. Res.-Sol. Ea., 115, B09215, doi:10.1029/2010JB007480, 2010.

Martini, F., Tassi, F., Vaselli, O., Del Potro, R., Martinez, M., del Laat, R. V., and Fernandez, E.: Geophysical, geochemical and geodetical signals of reawakening at Turrialba volcano (Costa Rica) after almost 150 years of quiescence, J. Volcanol. Geoth. Res., 198, 416–432, doi:10.1016/j.jvolgeores.2010.09.021, 2010.

Menyailov, I. A., Nikitina, L. P., Shapar, V. N., and Pilipenko, V. P.: Temperature increase and chemical change of fumarolic gases at Momotombo Volcano, Nicaragua, in 1982–1985: are these indicators of a possible eruption?, J. Geophys. Res.-Sol. Ea., 91, 12199–12214, doi:10.1029/JB091iB12p12199, 1986.

Moussallam, Y., Oppenheimer, C., Aiuppa, A., Giudice, G., Moussallam, M., and Kyle, P.: Hydrogen emissions from Erebus volcano, Antarctica, B. Volcanol., 74, 2109–2120, doi:10.1007/s00445-012-0649-2, 2012.

Oppenheimer, C.: Ultraviolet sensing of volcanic sulfur emissions, Elements, 6, 87–92, doi:10.2113/gselements.6.2.87, 2010.

Reagan, M., Duarte, E., Soto, G. J., and Fernandez, E.: The eruptive history of Turrialba volcano, Costa Rica, and potential hazards from future eruptions, in: Volcanic Hazards in Central America, vol. 412, edited by: Rose, W. I., Bluth, G. J. S., Carr, M. J., Ewert, J. W., Patino, L. C., and Vallance, J. W., Geological Soc Amer Inc, Boulder, 235–257, 2006.

Sawyer, G. M., Salerno, G. G., Le Blond, J. S., Martin, R. S., Spampinato, L., Roberts, T. J., Mather, T. A., Witt, M. L. I., Tsanev, V. I., and Oppenheimer, C.: Gas and

SED
6, 2293–2320, 2014

aerosol emissions from Villarrica volcano, Chile, J. Volcanol. Geoth. Res., 203, 62–75, doi:10.1016/j.jvolgeores.2011.04.003, 2011.
Shinohara, H., Giggenbach, W. F., Kazahaya, K., and Hedenquist, J. W.: Geological S. of J.: geochemistry of volcanic gases and hot springs of Satsuma-Iwojima, Japan: following Matsuo, Geochem. J., 27, 271–285, 1993.
Surono, Jousset, P., Pallister, J., Boichu, M., Buongiorno, M. F., Budisantoso, A., Costa, F., Andreastuti, S., Prata, F., Schneider, D., Clarisse, L., Humaida, H., Sumarti, S., Bignami, C., Griswold, J., Carn, S., Oppenheimer, C., and Lavigne, F.: The 2010 explosive eruption of Java's Merapi volcano – a "100-year" event, J. Volcanol. Geoth. Res., 241–242, 121–135, doi:10.1016/j.jvolgeores.2012.06.018, 2012.
Symonds, R. B., Rose, W. I., Bluth, G. J. S., and Gerlach, T. M.: Volcanic-gas studies; methods, results, and applications, Rev. Mineral. Geochem., 30, 1–66, 1994.
Symonds, R. B., Mizutani, Y., and Briggs, P. H.: Long-term geochemical surveillance of fumaroles at Showa-Shinzan dome, Usu volcano, Japan, J. Volcanol. Geoth. Res., 73, 177–211, doi:10.1016/0377-0273(96)00029-7, 1996.
Symonds, R. B., Gerlach, T. M., and Reed, M. H.: Magmatic gas scrubbing: implications for volcano monitoring, J. Volcanol. Geoth. Res., 108, 303–341, doi:10.1016/S0377-0273(00)00292-4, 2001.
Taran, Y. A., Hedenquist, J. W., Korzhinsky, M. A., Tkachenko, S. I., and Shmulovich, K. I.: Geochemistry of magmatic gases from Kudryavy volcano, Iturup, Kuril Islands, Geochim. Cosmochim. Ac., 59, 1749–1761, doi:10.1016/0016-7037(95)00079-F, 1995.
Vandaele, A. C., Simon, P. C., Guilmot, J. M., Carleer, M., and Colin, R.: SO_2 absorption cross section measurement in the UV using a Fourier transform spectrometer, J. Geophys. Res.-Atmos., 99, 25599–25605, doi:10.1029/94JD02187, 1994.
Vaselli, O., Tassi, F., Duarte, E., Fernandez, E., Poreda, R. J., and Huertas, A. D.: Evolution of fluid geochemistry at the Turrialba volcano (Costa Rica) from 1998 to 2008, B. Volcanol., 72, 397–410, doi:10.1007/s00445-009-0332-4, 2010.

SED
6, 2293–2320, 2014

Table 1. Spectral micro-window and all other parameter used for fitting the target gas species.

Day	Target gas	target gas Spectral window (cm^{-1})	Order of background polynomial	Species also included in the fit	Field of view (radiant)	Reference wavenumber (cm^{-1})	Volcanic gas pressure (hPa)	Volcanic gas temperature (K)	Atmospheric gas temperature (K)	Volcanic gas pathlenght (km)	Atmospheric pathlenght (km)	Notes
25 Mar 2013	SO_2	2440–2540	3	H_2O, CH_4, N_2O	0.45	2490	700 (for Turrialba summit)	450	295	0.002	0.35	FTIR to small incandescent 2012 vent
	CO_2	2020–2100	2	H_2O, CO	0.61	2060						
	H_2O	2020–2100	2	CO, CO_2	0.61	2060						
	HCl	2690–2830	3	H_2O, CH_4, N_2O	0.42	2750						
26 Mar 2013	SO_2	2440–2540	3	H_2O, CH_4, N_2O	0.45	2490	700 (for Turrialba summit)	300	290	0.03	0.035	FTIR to Lamp. South of 2010 vent
	CO_2	2020–2100	2	H_2O, CO	0.61	2060						
	H_2O	2020–2100	2	CO, CO_2	0.61	2060						
	CO	2020–2100	2	H_2O, CO_2	0.47	2150						
	HCl	2690–2830	3	H_2O, CH_4, N_2O	0.42	2750						

SED
6, 2293–2320, 2014

Table 2. X/SO_2 molar and mass ratios measured by FTIR spectroscopy and Multi-gas (for H_2) and gas composition of the mixed plume and 2012 vent. The inferred flux range of each species is based on an SO_2 flux estimate of 210.7 t day^{-1}.

Gas	Mixed Plume molar ratio (X/SO_2)	Mixed Plume mass ratio (X/SO_2)	Mixed Plume composition (mol%)	Infered flux (t day^{-1})	Infered flux (kg s^{-1})	2012 vent molar ratio (X/SO_2)	2012 vent composition (mol%)
H_2O	60.48	17.01	94.16	3583	41	57.72	86.69
CO_2	2.59	1.78	4.03	375	4	7.72	11.60
SO_2	1.00	1.00	1.56	211	2	1	1.50
HCl	0.15	0.09	0.23	18	0.20	0.14	0.21
CO	0.0021	0.0009	0.003	0.19	0.002	< DL	< DL
H_2	0.006	0.0002	0.009	0.04	0.0005	–	–

SED
6, 2293–2320, 2014

Table 3. Gas emission composition (in mole %) and molar ratio from several arc volcanoes. Data from Turrilaba – this study, Villarrica (Sawyer et al., 2011), Poas (Symonds et al., 1994), Momotombo (Menyailov et al., 1986), Masaya (Martin et al., 2010), Soufriere Hills (Hammouya et al., 1998), Mt St Helens (Gerlach and Casadevall, 1986), Kudryavy (Taran et al., 1995), Usu (Symonds et al., 1994), Showa-shinzan (Symonds et al., 1996), Satsuma Iwo Jima (Shinohara et al., 1993) and Merapi (Le Guern et al., 1982).

			Plume composition (mol %)						Molar ratio		
Arc volcanoes	Magma	Temperature (°C)	H_2O	CO_2	SO_2	H_2S	HCl	HF	H_2O/CO_2	SO_2/HCl	CO_2/SO_2
Turrialba (2013)	Basaltic andesite	> 800	94.16	4.03	1.56	–	0.2	–	23.4	7.8	2.6
Villarrica (2009)	Basaltic andesite	nm	90.54	5.69	2.59	< 0.01	0.87	0.3	15.9	3.0	2.2
Poas (1981)	Basaltic andesite	1045	96.69	1	1.46	0.01	0.75	0.09	96.7	1.9	0.7
Momotombo (1985)	Basalt	860	92.93	4.61	0.88	0.98	0.59	0.02	20.2	1.5	5.2
Masaya (2009)	Basalt	nm	93.6	4.01	1.49	–	0.74	0.17	23.3	2.0	2.7
Soufriere Hills (1996)	Andesite	720	95.9	2	0.36	0.03	1.72	–	48.0	0.2	5.6
Mt. St. Helens (1980)	Dacite	802	92.42	7.01	0.21	0.36	–	–	13.2		33.4
Kudryavy (1991)	Basaltic andesite	910	94.7	2.4	1.56	0.51	0.75	0.08	39.5	2.1	1.5
Usu (1979)	Dacite	676	96.4	2.65	0.22	0.54	0.16	0.03	36.4	1.4	12.0
Showa-Shinzan (1957)	Dacite	791	99.54	0.39	0.02	0.001	0.05	0.02	255.2	0.4	19.5
Satsuma Iwo Jima (1990)	Rhyolite	877	97.97	0.32	0.92	0.07	0.68	0.03	306.2	1.4	0.3
Merapi (1979)	Andesite	915	89.91	7.16	1.16	1.13	0.6	0.04	12.6	1.9	6.2

SED
6, 2293–2320, 2014

Figure 1. Location map showing Turrialba volcano at the southern tip of the Cordillera Central volcanic belt.

SED
6, 2293–2320, 2014

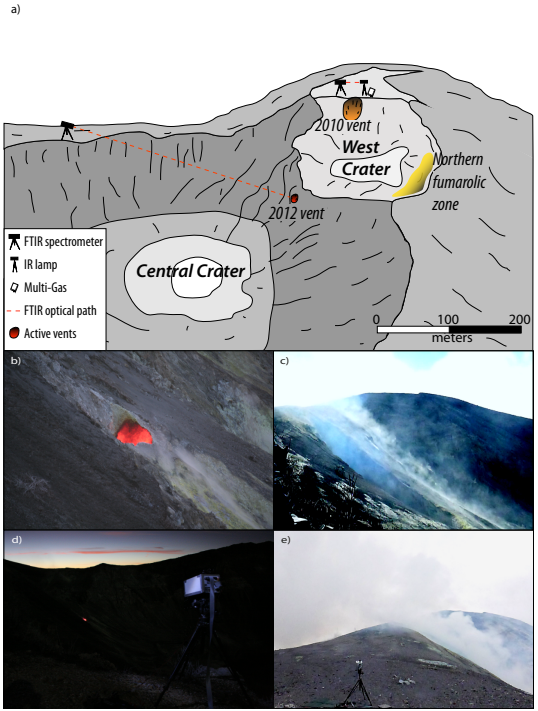

Figure 2. (a) Summit area of Turrialba looking due south, showing (not drawn to scale) the location of the three main vents and fumarolic fields together with the various locations of the FTIR spectrometer and "multi-gas" instrument. **(b)** Close up view of the 2012 vent at sunset. **(c)** Close up view of the 2010 vent. **(d)** Picture of the instrumental setup on 25 March 2013 with the FTIR spectrometer pointing at the 2012 vent (courtesy of Kayla Iacovino). **(e)** Picture of the instrumental setup on 26 March 2013 with the FTIR spectrometer pointing at an infrared lamp across the wind-blown mixed plume directly south of the 2010 vent.

SED
6, 2293–2320, 2014

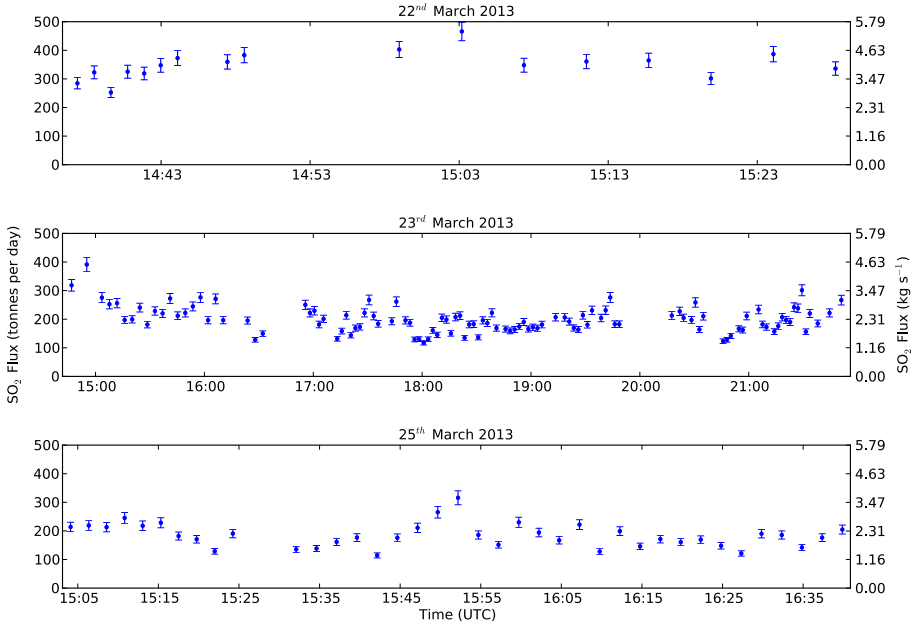

Figure 3. SO_2 fluxes shown in $t\,day^{-1}$ and $kg\,s^{-1}$ for three days of observations using DOAS horizontal scanning directly above the summit from a fixed observation point 2.0 km away (horizontal distance) from the summit. Only cloud-free periods with scans clearing the plume on both sides are reported.

SED
6, 2293–2320, 2014

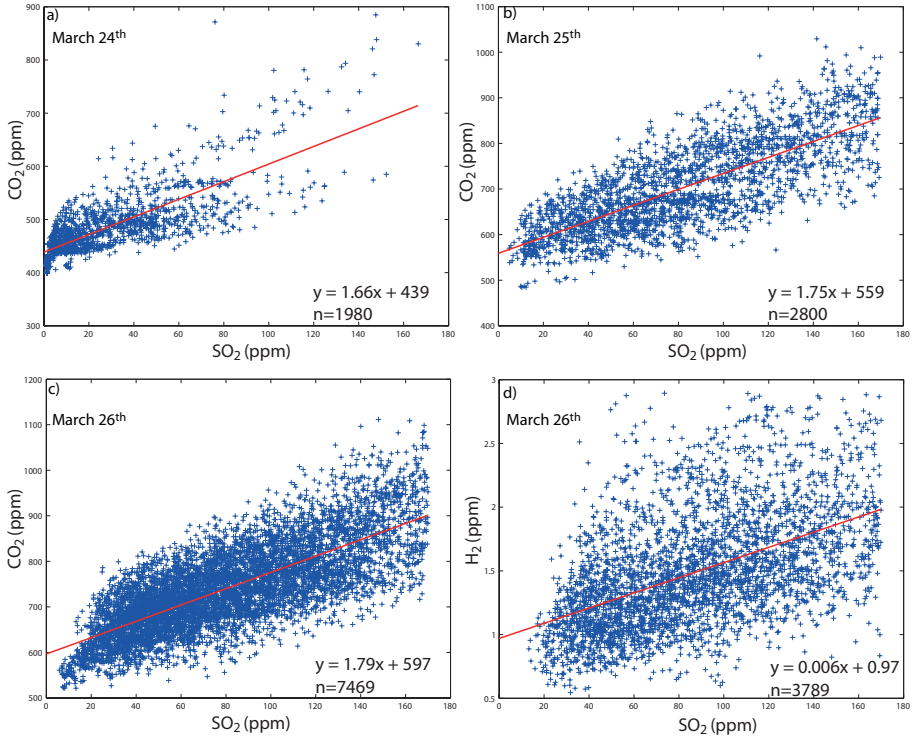

Figure 4. CO_2 vs. SO_2 and H_2 vs. SO_2 scatter plots from three days of sampling of the Turrialba mixed plume, directly south of the 2010 vent. **(a)** 17:52 to 18:58, 24 March 2013, UTC. **(b)** 20:24 to 21:57, 25 March 2013, UTC. **(c)** 22:05, 25 March 2013 to 02:14, 26 March 2013, UTC. **(d)** 00:10 to 02:14, 26 March 2013, UTC. Regression lines are shown in red and corresponding parameters are displayed on the lower right corner of each plot

SED
6, 2293–2320, 2014

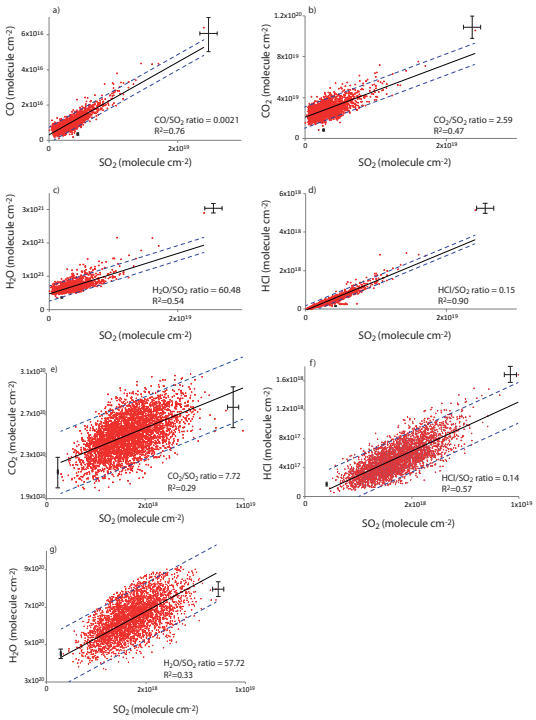

Figure 5. Scatter plots showing column amounts of each volcanic gas species vs. SO_2. Upper four scatter plots show data acquired on 26 March 2013 sampling of the Turrialba mixed plume, directly south of the 2010 vent using a IR lamp as source and a 35 m path length. **(a)** CO, **(b)** CO_2, **(c)** H_2O, **(d)** HCl. Lower three scatter plots show data acquired on 25 March 2013 sampling the 2012 vent using incandescence from the vent as the IR source and a 350 m path length. **(e)** CO_2, **(f)** HCl, **(g)** H_2O. The y-axis offsets seen in **(b)** and **(e)** and **(c)** and **(g)** represent the atmospheric background column amounts of CO_2 and H_2O respectively. Dashed lines show prediction bands at 95 % confidence level.

SED
6, 2293–2320, 2014

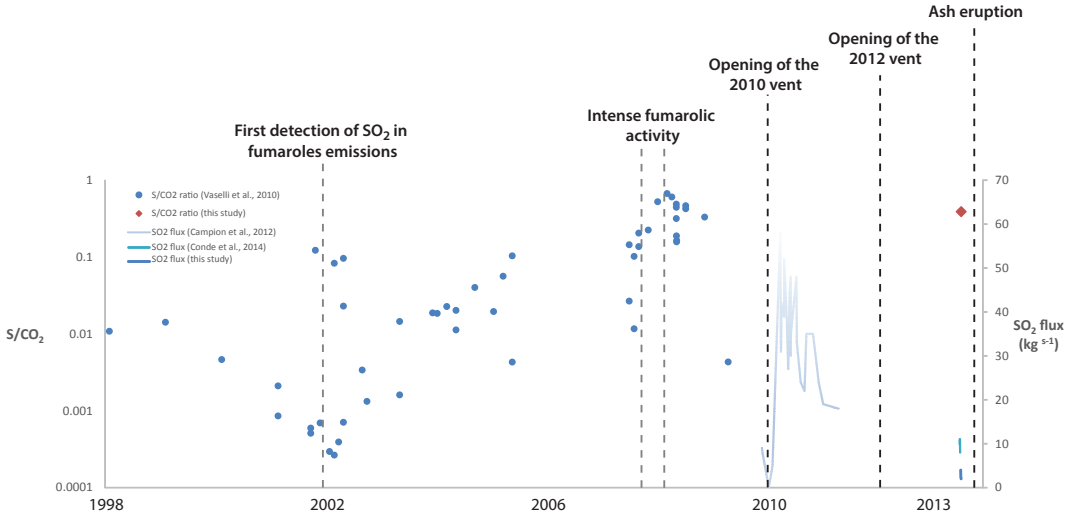

Figure 6. Time series showing the observed evolution of gas emissions in term of S/CO_2 ratio and SO_2 flux from 1998 to 2013 using data from Vaselli et al. (2010), Campion et al. (2012) and this study. Important events such as vent opening during phreatic eruptions are noted.

SED
6, 2293–2320, 2014

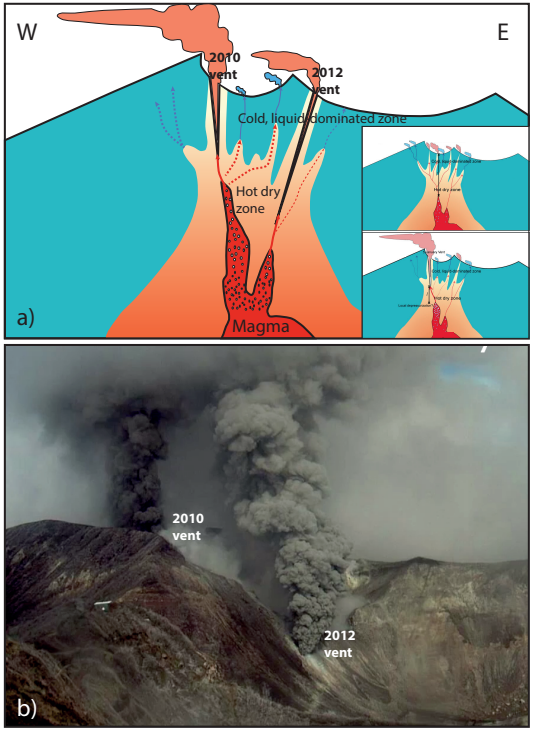

Figure 7. (a) Schematic cross section representation of the summit area of Turrialba at the time of writing. The figure is drawn after the style of Fig. 7 in (Campion et al., 2012) (reproduced as inset) showing the progression of the "Hot dry zone" since the opening of the 2012 vent. The figure also represents the 2012 vent linked at a slightly deeper level than the 2010 vent as to explain the difference in gas ratios (see text). **(b)** Photograph from the Turrialba webcam taken on 21 May 2013 showing the most recent ash eruption in which both vents erupted simultaneously.

SED
6, 2293–2320, 2014